Redox-Induced Conformational Changes in Plastocyanin: An Infrared Study†

Stefka G. Taneva,‡ Ulrike Kaiser,§ Anthony A. Donchev,|| Mitko I. Dimitrov,|| Werner Mäntele,§,⊥ and Arturo Muga*,‡

Unidad de Biofísica (CSIC-UPV/EHU) y Departamento de Bioquímica, Universidad del País Vasco, Aptdo. 644, 48080 Bilbao, Spain, Institut für Physikalische und Theoretische Chemie, Universität Erlangen−Nürnberg, D-91058 Erlangen, Germany, and Institute of Biophysics, Bulgarian Academy of Sciences, Sofia 1113, Bulgary

Received February 16, 1999; Revised Manuscript Received May 18, 1999

ABSTRACT: The conformational changes associated with the redox transition of plastocyanin (PC) were investigated by absorption and reaction-induced infrared spectroscopy. In addition to spectral features readily ascribed to β and turn protein secondary structures, the amide I band shows a major component band at 1647 cm^{-1} in both redox states of the protein. The sensitivity of this component to deuteration and increasing temperature suggests that PC adopts an unusual secondary structure in solution, which differs from those described for other type I copper proteins, such as azurin and halocyanin. The conformations of oxidized and reduced PC are different, as evidenced (*1*) by analysis of their amide I band contour and the electrochemically induced oxidized-minus-reduced difference spectrum and (*2*) by their different thermal stability. The redox-induced difference spectrum exhibits a number of difference bands within the conformationally sensitive amide I band that could be assigned to peptide C═O modes, in light of their small shift upon deuteration, and to signals attributable to side chain vibrational modes of Tyr residues. Lowering the pH to 4.8 induces destabilization of both redox states of the protein, more pronounced for reduced PC, without significantly affecting their secondary structure. Besides the conformational differences obtained at neutral pH, the oxidized-minus-reduced difference spectrum shows two broad and strong negative bands at 1405 and 1571 cm^{-1}, assigned to COO^- vibrations, and a broad positive band at 1710 cm^{-1}, attributed to the C═O vibration of a COOH group(s). These bands are indicative of a protonation of (an) Asp or Glu side chain(s) upon plastocyanin oxidation at acidic pH.

Plastocyanin (PC)[1] is a 10.5 kDa "blue copper" type I protein that functions on the luminal side of the thylakoid membrane as a mobile electron carrier between cytochrome b_6/f and photosystem I (*1*, *2*). Due to its location, PC should experience upon illumination a decrease in pH of about 2−3 units (*3*). Therefore, pH could modulate the conformation and activity of PC, in this way acting on the photosynthetic electron transport. The crystal structure of oxidized and reduced PC from poplar has been determined at several pH values (*4*, *5*). The protein consists of a single polypeptide chain of 99 residues, forming an 8-stranded β-sandwich, with a single copper ion coordinated by 2 sulfurs from Cys 84 and Met 92, and 2 δ-nitrogens from His 37 and His 87. From a functional point of view, the most interesting aspects of the crystallographic data are the following: (*1*) the geometry of the copper center of reduced PC differs significantly from that of the oxidized protein; (*2*) the sensitivity to pH of the Cu-site geometry depends on the redox state of the protein, only that of reduced PC being affected upon decreasing the pH; and (*3*) despite the oxidation state of the copper atom and/or the pH of the surrounding medium, the conformation of the protein is not substantially affected and its overall fold remains essentially unaltered.

However, these data do not rule out the possibility that localized regions of the protein molecule, other than the Cu site, may undergo redox- and pH-dependent conformational changes that could modulate the function of PC. In fact, near-UV absorption and circular dichroism studies have shown that the extinction coefficient and ellipticity values are sensitive to both the redox state of the protein and the pH of the medium (*6*, *7*). Interestingly enough, in both cases the observed changes could be ascribed, at least in part, to conformational changes around the solvent-exposed and functionally significant Tyr 83 (*8*).

The aim of this study is to evaluate the effect of pH and redox state on the conformational properties of PC in solution. Furthermore, in an attempt to understand the microheterogeneity of the primary structure of electron carriers (*9*), these studies have been carried out on two naturally occurring PC variants from poplar, namely, PCa and PCb. PCb, as compared to PCa, has 12 amino acid

† This work was supported by grants from the University of the Basque Country (A.M.; EB 200/96, GO3/98), DGICYT (A.M.; PB97-1225), and Basque Government (EX98/28). S.G.T. is a recipient of a fellowship from the Basque Government. W.M. and U.K. were supported by the Deutsche Forschungsgemeinschaft (Ma 1054/9-1 and /9-2).

* Corresponding author. Phone: +34-94-46012624; Fax: +34-94-4648500; E-mail: gbpmuvia@lg.ehu.es.

‡ Universidad del País Vasco.

§ Universität Erlangen−Nürnberg.

|| Bulgarian Academy of Sciences.

⊥ Present address: Institut für Biophysik, Johann Wolfgang Goethe Universität, Theodor Stern Kai 7, D-60590 Frankfurt, Germany.

[1] Abbreviations: E_m, midpoint redox potential; IR, infrared spectroscopy; PC, plastocyanin; RIDS, redox-induced difference spectroscopy; SHE, standard hydrogen electrode; T_m, midpoint denaturation temperature.

10.1021/bi990376t CCC: $18.00
Published on Web 07/08/1999

replacements which have been suggested to be important in determining their redox and electrochemical properties (*9*). We have used Fourier transform infrared (IR) spectroscopy to compare both the secondary structure and the thermal stability of these PC species in solution, and combined the IR data with electrochemical titrations to characterize their redox potentials and conformational changes associated with the redox transition. From an experimental point of view, the great advantage of combining electrochemistry and infrared spectroscopy is that there is no need for weighted subtractions or data treatment procedures.

MATERIALS AND METHODS

Sample Preparation. PCa and PCb were purified from fresh leaves of poplar *Populus nigra* var. *Italica* according to Dimitrov et al. (*9*), and stored at −20 °C in 60 mM phosphate buffer, pH 7.0. For IR spectroscopy, the protein was concentrated to approximately 1−2 mM using Ultrafree-MC filters (Millipore). Oxidized and reduced PC were prepared by treatment with 5 mM potassium ferricyanide and ascorbic acid, respectively. Exchange of buffer and of H_2O by D_2O (99.8% purity, Sigma) was carried out by repeatedly washing the sample in the desired H_2O- or D_2O-based buffers, equilibrating overnight at 4 °C, and concentrating the protein.

Infrared (IR) Transmission Spectroscopy. Samples for IR spectroscopy were equilibrated in 60 mM phosphate, pH 7.0, or 60 mM cacodylate buffer, pH 4.8. The use of cacodylate buffer provided an open window in the 1750−1400 cm^{-1} spectral region under acidic pH, and avoided the need of organic acid containing buffers which produce IR signals (around 1715, 1565, and 1400 cm^{-1}) that would overlap with protein vibrations (see below). The slow tendency of the reduced proteins to self-associate in cacodylate was avoided in the presence of 200 mM $Na_2(SO_4)$, which does not substantially modify the stability and redox properties of PC (data not shown). Due to the low buffer capacity of cacodylate, the pH of each sample was adjusted to 4.8 prior to concentration. Thermal stability and VIS titration measurements were also repeated in 60 mM phosphate/citric acid, pH 4.8, giving essentially the same results as those obtained in cacodylate buffer. IR spectra were recorded with a Nicolet 520 (D_2O samples) or a Nicolet Magna (H_2O samples) spectrophotometer, both equipped with MCT detectors. Samples were placed in a thermostated cell between two CaF_2 windows separated by 50 μm (D_2O samples) and 6 μm (H_2O samples). A total of 1000 scans were accumulated, at 2 cm^{-1} resolution, for each spectrum. Thermal studies were carried out by a step-heating method with 3 °C steps, leaving the sample to stabilize for 5 min before recording the spectra. During data acquisition, the temperature was monitored with a thermocouple in contact with the windows and was stable within 0.3 °C. Solvent subtraction, Fourier self-deconvolution, and band position determination were performed as described previously (*10*).

Redox-Induced IR Difference Spectroscopy (RIDS). The optically transparent thin-layer electrochemical cell used for difference spectroscopy was described previously (*11*). The 15 mm diameter gold grid working electrode was surface modified by dipping it in a solution of 1 mM pyridine-3-carboxaldehyde thiosemicarbazone (PATS-3), as described by Hill et al. (*12*). After 10 min, excess PATS-3 was thoroughly removed with deionized water, and the gold grid was dried. The reaction mixture consisted of 1.6−3.0 mM purified PC solution in 100 mM phosphate (pH/pD 7.0) or cacodylate [pH/pD 4.8; 200 mM $Na_2(SO_4)$] buffer, containing 100 mM KCl as conducting electrolyte. To accelerate the reaction, redox mediators (*13*) were added to a final concentration of 50 μM. The path length was set to 5−8 μm, to ensure sufficient transmission in the 2000−1000 cm^{-1} range. Under these experimental conditions, the redox mediators did not contribute to the difference spectra. The potential was controlled by a potentiostat built to our design (Model Sevenich-Gimbel type I). The experimental setup integrated a dispersive visible (VIS) spectrometer for the 400−900 nm range into a modified Bruker IFS 25 FTIR spectrophotometer equipped with an MCT detector (*14*). IR and VIS difference spectra as a function of the applied potential were obtained simultaneously for each sample, which guaranteed identical experimental conditions [path length, temperature (5 °C), protein concentration] for each potential. The possibility of recording in the same experiment the VIS and IR spectra of the sample allowed the normalization of the difference signals so that comparison between different samples, in our case PCa and PCb, became feasible. The VIS photometer and the potentiostat were controlled by data acquisition and treatment software (MSPEK) developed by S. Grzybek in W Mäntele's laboratory.

Potentiometric Titrations. A series of potentials (30 mV steps) in the range 50−700 mV were applied to the spectroelectrochemical cell. Fast, quantitative, and reversible redox reactions were obtained at the gold grid working electrode for both PCa and PCb. After equilibration of the cell contents at each potential, a VIS spectrum from 400 to 900 nm and an IR spectrum from 2000 to 1000 cm^{-1} were recorded. Equilibration was followed by monitoring the electrode current and by recording VIS spectra till no further changes were observed. Under our experimental conditions, equilibration took between 0.5 and 1.5 min. Difference spectra were calculated directly from the single-beam spectra, the spectrum at the lowest (highest) potential being the reference for the oxidative (reductive) cycle. No baseline subtractions, weighted subtractions, or data treatment procedures were performed. A plot of the amplitude of the difference bands in the VIS and IR regions against the applied potential allowed fitting of the experimental data to a calculated Nernst curve assuming a single redox-active component. The fit yielded the electrochemical characteristics of the proteins: the midpoint potential (E_m) and the number of electrons (n) transferred. All potentials quoted refer to the standard hydrogen electrode (SHE) and are within ca. 5 mV precision.

RESULTS

Infrared Absorption Spectroscopy. The 1750−1500 cm^{-1} spectral region of the IR spectra of oxidized (upper traces) and reduced (bottom traces) PCa, recorded at neutral pH in H_2O- and D_2O-based buffers, is shown in Figure 1. The most prominent features of the original spectra are the amide I (1647 cm^{-1}) and amide II (1553 and 1533 cm^{-1}) bands (data not shown). The amide I band (1700−1615 cm^{-1}) contains contributions from the different secondary structure elements, which give rise to a composite band enclosing the structural

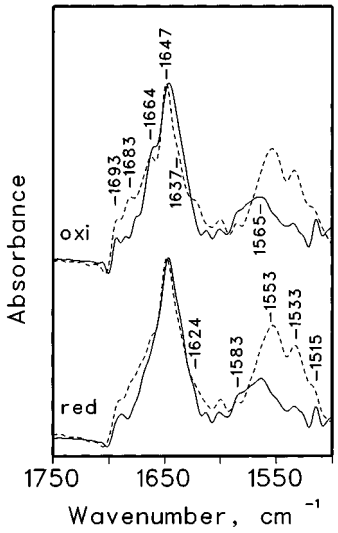

FIGURE 1: Deconvoluted infrared spectra of oxidized (top) and reduced (bottom) PCa in H_2O (- - -) and D_2O (—) buffers. The spectra were recorded at 25 °C, in 60 mM phosphate buffer, pH or pD 7.0. Protein concentration was 2 mM. Deconvolution was performed using a Lorentzian with a half-bandwidth of 18 cm^{-1} and a band-narrowing factor of 2.

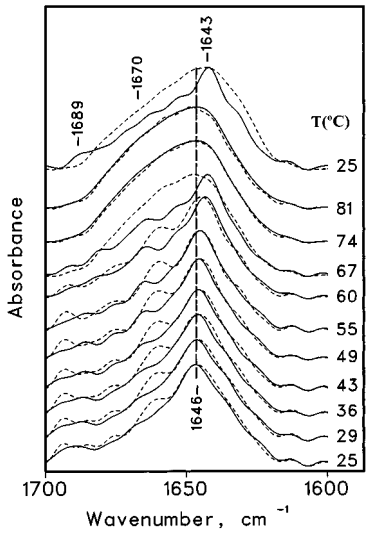

FIGURE 2: Temperature dependence of the IR spectra of oxidized (- - -) and reduced (—) PCa. Deconvoluted spectra in the amide I region recorded at increasing temperatures, and after cooling the sample to 25 °C (top traces). Measurements were performed using a step-heating method, described under Materials and Methods, on samples containing 2 mM PC, 60 mM phosphate, pD 7.0. The deconvolution parameters were the same as in Figure 1.

information of the protein (*15*). After self-deconvolution, its fine structure reveals several components that are downshifted by ≈2−6 cm^{-1} upon deuteration (Figure 1). These band components are usually assigned to different secondary structures on the basis of theoretical and experimental studies (*15*−*18*).

In H_2O buffer, the deconvolved spectrum of oxidized PCa shows five bands attributable to protein backbone structure. The band at 1637 cm^{-1} has been assigned to β structures. The assignment of the major component at 1647 cm^{-1} appears to be somewhat less unequivocal, and will be discussed in light of the thermally induced changes in the protein IR spectrum. Note that its position is downshifted by only 1−2 cm^{-1} upon deuteration. The band at 1664 cm^{-1} (H_2O) and 1661 cm^{-1} (D_2O) has been attributed to turn structures. These, together with the high-frequency component of antiparallel β structure, are associated with the component bands at 1683 and 1693 cm^{-1}. Reduction of PCa does not significantly modify the major features of the IR spectrum of the protein, although a decrease in the relative intensity of the 1664 (H_2O), 1661 cm^{-1} (D_2O), component is evident and will be discussed in combination with RIDS results (see below). The drastic reduction in the intensity of the amide II band (1553 and 1533 cm^{-1}), as a consequence of isotopic substitution of exchangeable NH protons by D, indicates a high degree of solvent accessibility of the protein backbone. The persisting bands are proposed to be due to amino acid side chain absorptions: tyrosine (1515 and 1614 cm^{-1}), glutamate (1565 cm^{-1}), and aspartate (1583 cm^{-1}) (*19*).

A comparison between the IR spectra of both redox states of PCa and PCb shows that the 12 substitutions in the primary structure of the protein have very little effect on its conformation, and that both sequences adopt a similar fold in solution (data not shown). At pH 4.8, their IR spectra are comparable to those described at neutral pH, with regard to the position and relative intensities of the amide I band components (data not shown).

Temperature-Induced IR Spectroscopy. To further characterize the conformation of the reduced and oxidized forms of these two naturally occurring PC sequences, we have investigated their redox-dependent thermal stability. The effect of temperature on the amide I band of reduced and oxidized PCa in D_2O buffer is shown in Figure 2. The spectra of reduced PCa measured between 25 and 55 °C are similar to each other, although the relative intensity of the minor component at 1665 cm^{-1} gradually increases with temperature. A further increase in temperature to 67 °C induces a shift of the major amide I band component to 1643 cm^{-1}, and a reorganization of the turn structures as evidenced by changes in the position and intensity of the band components above 1660 cm^{-1}. Interestingly, these spectral changes are not observed for the oxidized form of the protein at pretransition temperatures (i.e., below 60 °C; see below). The pronounced changes in the IR spectra of oxidized and reduced PCa above 60 °C and 67 °C, respectively, demonstrate that heating above these temperatures causes major structural changes in both redox states of the protein. The spectra of the thermally denatured proteins are very similar and exhibit a broad, asymmetric amide I band centered at around 1650 cm^{-1} with a shoulder at. 1670 cm^{-1}. A similar amide I band contour has been described for thermally denatured RNase T1, and it was associated with predominantly, but not completely, irregular protein structures which still retained turn-like structures (*20*).

After cooling the thermally denatured samples to 25 °C, the IR spectrum of the oxidized form of the protein remains almost featureless as compared to that of reduced PCa (Figure 2, top traces). The latter shows the fine structure characteristic of the native protein, although the positions of its component bands are closer to those described for the protein at 67 °C. More detailed information on the thermally induced conformational changes can be obtained by plotting the bandwidth (Figure 3A) and position (Figure 3B) of the amide I band as a function of temperature. Both parameters show that thermal denaturation of reduced, but not of oxidized, PCa proceeds

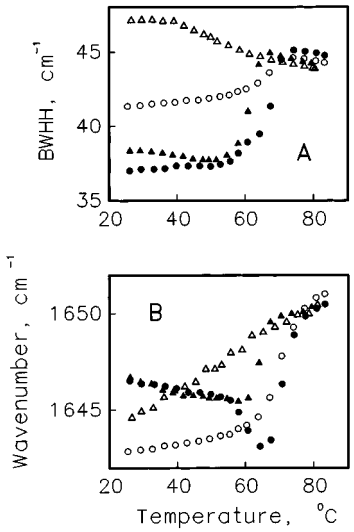

FIGURE 3: Thermal stability of PC. Temperature dependence of the bandwidth at half-height (BWHH) (A) and the absorption maximum (B) of the amide I band of oxidized (triangles) and reduced (circles) PC. The samples were subjected to a first heating cycle (filled symbols), and after equilibration at 25 °C until a stable signal was reached to a second one (empty symbols).

Table 1: Effect of Redox State and pH on the Thermal Stability of PCa and PCb: Midpoint Denaturation Temperature (°C) for the Overall Unfolding of Reduced and Oxidized PCa and PCb at pH 7.0 and 4.8[a]

	PCa		PCb	
pH	reduced	oxidized	reduced	oxidized
7.0	66.7	61.8	64.9	62.4
4.8[b]	47.2	48.2	46	53

[a] These values are the average of at least two independent determinations on two different protein batches. [b] To avoid temperature-induced pH alterations, these samples were measured in 60 mM cacodylate, 200 mM $Na_2(SO_4)$ and in 60 mM phosphate/citric acid. The T_m values obtained in both buffers were comparable, with a maximum standard deviation of ±1 °C. Reduction of both sequences with dithionite or ascorbic acid gave similar values.

through a distinguishable intermediate conformation. Reheating of the reduced protein shows a denaturation transition within the same temperature range observed for the native protein, suggesting that the reduced protein regains, at least partially, a native-like secondary structure after thermal denaturation. Supporting this interpretation is the fact that the absorption band at 598 nm characteristic of native, oxidized PC develops to about 50% of the initial value after addition of excess ferricyanide to the previously thermally denatured, reduced protein (data not shown). None of these effects are observed with the oxidized protein (Figure 3). Essentially the same temperature-induced effect on the IR spectra was observed for the reduced and oxidized forms of PCb (data not shown). The midpoint transition temperatures of the unfolding process estimated from "melting curves", as shown in Figure 3A (*21*), of both redox states of PCa and PCb are summarized in Table 1.

To detect subtle differences between the unfolding pathways of the reduced and oxidized forms of PC, we have analyzed the temperature-induced IR difference spectra. Positive and negative features in these spectra reflect fine structural differences between conformations obtained at consecutive temperatures (every 3 °C) during the heating

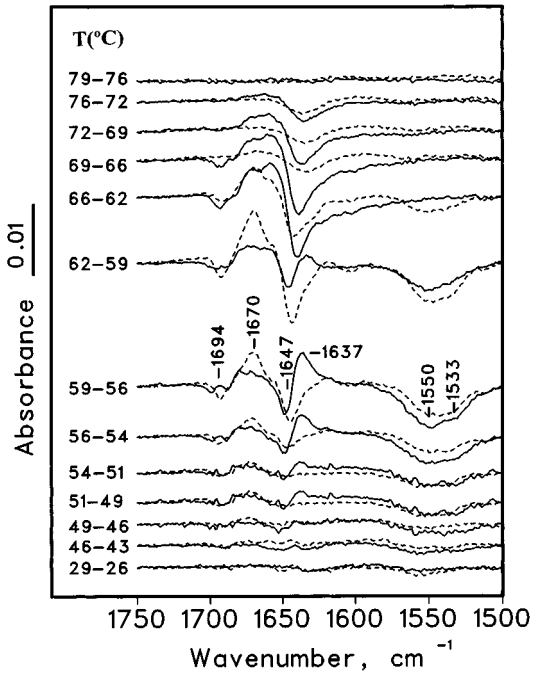

FIGURE 4: Temperature-induced difference spectra of oxidized (- - -) and reduced (—) PCa. The spectra were obtained by subtracting two original ones measured at consecutive temperatures. Protein concentration was 2 mM in 60 mM phosphate, pD 7.0.

procedure, in whose absence a roughly flat line is obtained (Figure 4). There are clear spectral differences in the 56−66 °C temperature range between oxidized and reduced PC. The thermal unfolding of the former shows one conformational transition which is characterized by the presence in the difference spectra of negative bands at 1694 and 1644 cm^{-1} which, together with a broad positive band at 1670 cm^{-1}, are indicative of structural rearrangements in irregular and turn structures (Figure 4, dashed lines). The development of a negative broad band with two minima at around 1550 and 1533 cm^{-1}, within the same temperature interval where the above difference spectral features appear, reflects the deuteration of the rather small fraction (approximately 15%) of NH groups that remained unexchanged in the native protein. In contrast, the unfolding pathway of reduced PC shows two distinguishable thermotropic events (Figure 4, solid lines). The first one occurs between 56 and 62 °C, and is characterized by the appearance of a negative band at 1647 cm^{-1}, and positive bands at 1694, and around 1670 and 1637 cm^{-1}. The latter band was absent in the difference spectra of the oxidized protein, and might represent the formation of an intermediate in the thermal unfolding pathway of reduced PC. It is important to note that during this first thermal event the amide I band retains its structured shape (see Figure 3), while the polypeptide backbone becomes accessible to the solvent (see the broad negative band with minima at 1550 and 1533 cm^{-1}). The second thermal event (66−76 °C) most likely represents a more extensive unfolding of the protein.

Acidification of the medium induces an overall destabilization of the protein structure, as evidenced by a decrease of the T_m values of both PCa and PCb, regardless of their redox state (Table 1). The effect is more pronounced for reduced (ΔT = 19.5 and 18.9 °C for PCa and PCb, respectively) than for oxidized (ΔT = 13.6 and 10 °C for PCa and PCb, respectively) PC. A comparison of both

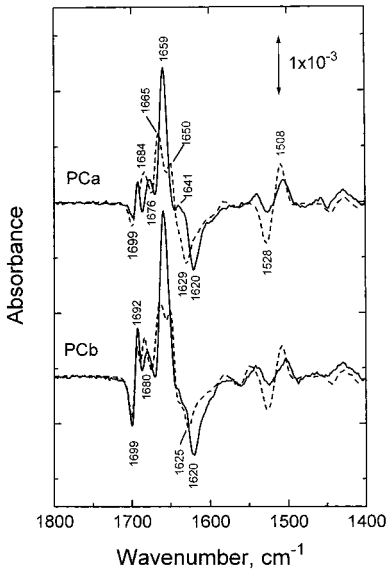

FIGURE 5: Oxidized-minus-reduced IR difference spectra of PCa (top) and PCb (bottom) recorded in H_2O (- - -) and D_2O (—) buffers. Measurements were performed on samples containing 2 mM plastocyanin at neutral pH/pD, at 5 °C. The potential was switched from 150 to 630 V over several cycles. Positive and negative bands are associated with the oxidized and reduced states, respectively.

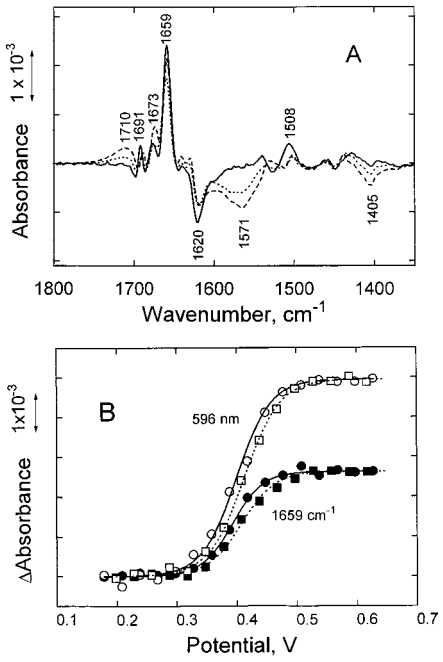

FIGURE 6: Effect of pH on the redox-dependent IR difference spectra and redox potential of PC. (A) Oxidized-minus-reduced spectra of PCa at pD 7.0 (—), 4.8 (•••), and 3.6 (- - -). Protein concentration was 2 mM. Buffers were 100 mM phosphate, pD 7.0, or 100 mM cacodylate, 200 mM $Na_2(SO_4)$, pD 4.8 and 3.6. The pH of the samples under acidic conditions was adjusted by the addition of HCl. (B) Redox titration of the VIS 598 nm (empty symbols) and IR 1659 cm^{-1} (filled symbols) absorbance bands of PCa, at pH 7.0 (circles) and 4.8 (squares). The solid and dashed lines represent the calculated Nernst functions, with n and E_m values given in the text, at neutral and acidic pH, respectively.

sequences reveals that while the pH-induced destabilization is similar for their reduced forms, the oxidized state of PCb is more stable against the thermal challenge at low pH. Under these experimental conditions, the unfolding pathway of both redox forms is similar and, in contrast to what was found at neutral pH, the IR spectrum of the unfolded forms is dominated by a band component at 1620 cm^{-1} which indicates extensive aggregation of the thermally denatured protein molecules (data not shown).

Reaction-Induced Difference Spectroscopy (RIDS). The oxidized-minus-reduced IR difference spectra of PCa recorded in H_2O- and D_2O-based buffers at pH/pD 7.0 are shown in Figure 5. They were calculated from two single-beam spectra measured after equilibration of the cell content at 630 mV (oxidized sample) and 150 mV (reduced sample). When the subtraction is performed in this way, positive and negative bands are associated with the oxidized and reduced forms, respectively. In H_2O buffer, the strongest signals appear within the amide I band (1700−1600 cm^{-1}) spectral region: a differential signal at 1699(−)/1692(+) cm^{-1}; three positive bands at 1684, 1665, and 1650 cm^{-1}; and a negative band at 1629 cm^{-1}. Equilibration of PCa in D_2O results in band shifts of 1−9 cm^{-1} toward lower wavenumbers. The difference signal is shifted by 1 cm^{-1}, the two positive bands are downshifted to 1676 and 1659 cm^{-1}, and the negative band to 1620 cm^{-1}. The corresponding band of the 1650(+) cm^{-1} signal is not observed in the D_2O spectrum, and instead a weak shoulder appears at 1641 cm^{-1}. The amide II region is characterized by one major difference signal at 1528(−)/1508(+) cm^{-1}, which is found downshifted by 2 cm^{-1} upon deuteration.

The band pattern of the oxidized-minus-reduced difference spectra of PCb is very similar to that described for PCa (Figure 5; bottom spectra). Band positions differ by no more than 2 cm^{-1} in H_2O and 4 cm^{-1} in D_2O. While most of the relative band intensities are alike for both proteins, those of the 1699(−)/1692(+) cm^{-1} and 1650(+) cm^{-1} signals are higher for PCb. The former difference is maintained in D_2O, while the latter band also disappears upon deuteration. It should also be noted that the 1684 cm^{-1} positive signal shows a smaller downshift upon deuteration for PCb (to 1680 cm^{-1}) than for PCa (to 1676 cm^{-1}).

The structural rearrangement associated with the redox transition of PCa and PCb at neutral pH occurs also at pH 4.8. However, at low pH, besides the band pattern described at pH 7.0 the difference IR spectra display a broad positive band centered at around 1720 cm^{-1}, and two negative bands at 1564 and 1410 cm^{-1} (data not shown). The redox induced difference spectra of PCa at pD 7.0 and pD 4.8 as well as the spectrum of an unbuffered sample at pD 3.6 are compared in Figure 6A. It should be mentioned here that unbuffered samples at acidic pH/pD exhibit a redox reaction as reversible and complete as buffered samples. Their use allows us to rule out any possible interference from the buffer (*22*). In addition to the conserved band pattern already described for pD 7.0, three bands emerge at pD 4.8 which correspond to the additional bands observed at pH 4.8. The positive band is centered at about 1710 cm^{-1}, although its exact location is difficult to determine due to overlapping with the 1699(−)/1691(+) cm^{-1} difference signal, and the two negative bands appear at 1571 and 1405 cm^{-1}. The band patterns of all the experiments performed at pD ≤ 4.8 (including pD 3.9; data not shown) are similar, although the following significant differences appear as the pH is lowered: (i) the intensity of the three bands mentioned above increases; (ii) the positive signal at 1676 cm^{-1} (pD 7.0 and 4.8) is downshifted to 1674 cm^{-1} while its relative intensity

increases (pD 3.6); and iii) the intensity of the positive signal at 1508 cm^{-1} (pD 7.0) is significantly reduced and its position is displaced to 1506 cm^{-1} (pD 4.8 and 3.6). An identical pH-dependent behavior was observed for the difference IR spectra of PCb, reinforcing the similarity of the redox-dependent conformational changes for both plastocyanin sequences (data not shown).

Finally, the redox midpoint potentials for PCa and PCb were estimated from titration experiments, as previously reported (*22*). Application of intermediate potentials between 150 and 630 mV led to titration of both the 600 nm absorption band and the IR difference signals (Figure 6B). The changes in amplitude of all bands could be closely approximated by a Nernst curve calculated assuming a single redox-active component and a number (*n*) of electrons transferred varying from 0.85 to 1.05. The E_m values (vs SHE) calculated for PCa and PCb at neutral pH were 391 and 392 mV, respectively, whereas at pH 4.8 their values were 415 and 410 mV, in agreement with results obtained from spectrophotometric titrations of PC with ferricyanide (data not shown). The experimentally observed small pH dependence of E_m is remarkably different from that described for other small copper proteins, such as halocyanin and azurin (*22*, *23*).

DISCUSSION

Conformation and Thermal Stability of Reduced and Oxidized PCa and PCb. The absorption maximum of the amide I band of β proteins is typically located in the 1640−1620 cm^{-1} frequency range (*17*, *18*). In this context, the IR spectra of PCa and PCb are unusual as compared to the well-characterized infrared signals of other mainly β polypeptides, including type I copper proteins such as azurin and halocyanin whose absorption maxima appear at 1636 (*24*) and 1630 cm^{-1} (*22*), respectively. The band components detected within the 1640−1620 cm^{-1} spectral region in the deconvoluted spectra of both PC sequences indicate that a significant proportion ($\approx$26 $\pm$ 5% of the total amide I band intensity) of residues are involved in β-strands. The assignment of the strongest band component (at $\approx$1647 cm^{-1}) is not straightforward and requires a comparison of the spectra recorded in H_2O and D_2O buffers. Its position in the latter medium (1646 cm^{-1}) is within the spectral region where vibrations from solvent-exposed, distorted α-helices and unordered structures appear. However, the following evidences argue against this putative assignment: (1) Deuteration normally shifts bands arising from unordered structures as much as 10 cm^{-1} toward lower wavenumbers, whereas this component is downshifted by no more than 2 cm^{-1}; (2) the presence of only two short α-helical segments (six residues) in the X-ray structure of PC could give rise to a weak absorption band that might overlap with the 1646 cm^{-1} component in D_2O and add to the unresolved region around 1655 cm^{-1} in H_2O; and (3) the absence of a component band in H_2O at 1657−1650 cm^{-1}, characteristic of unordered and helical conformations. Therefore, we conclude that none of these structures can significantly contribute to the intensity of the major absorption band component. Other possible contributions could come from side chain absorptions of Asn residues around 1680 (H_2O) and 1648 (D_2O) cm^{-1} (25). Assuming similar extinction coefficients for the C═O mode of these residues and the peptide C═O groups, the six and five Asn residues of PCa and PCb, respectively, could contribute to the intensity of the 1647 cm^{-1} component in D_2O by approximately 5−6%. Moreover, the similar relative intensity of this spectral feature in H_2O (37 $\pm$ 4%) and D_2O (41 $\pm$ 4%) further confirms the rather small contribution of Asn residues. Thus, the unusual location of the amide I absorption maximum of PC reflects an intrinsic conformational property of this protein.

The secondary structure estimate for poplar PC, based on its X-ray structure, is 35% β-strands and 6% 3_{10}-helix (*26*). The remaining residues fold into turns and irregular structures, and therefore they could account for at least part of the intensity of the 1646 cm^{-1} component. Absorption bands at similar positions have been described for other proteins that share the presence of irregular structures (loops, turns) connecting different secondary structure elements (*27*−*30*). The small downshift observed for this component upon deuteration (1−2 cm^{-1}) together with its sensitivity to the thermal denaturation of the protein suggests that the polypeptide segment(s) responsible for this absorption band is (are) an integral structural part of the protein 3-D structure. Especially interesting is the region spanning residues 42−68, which as seen by X-ray forms a long loop containing 4 β-turns and a short 3_{10}-helix (3 residues). Another factor that might account for the high intensity of this band component is related to the effect of unusual hydrogen bonding patterns on the location of the amide I (C═O stretching) frequency. Backbone C═O groups involved in β strands which could form weaker hydrogen bands would shift their corresponding vibration to higher frequencies. The twisted, interacting character of the mixed β structure of PC that results in an unusual far-UV CD spectrum (*6*) would favor this situation.

The similarity between the secondary structures of both PC sequences extends to the thermal unfolding pathway of their oxidized and reduced forms. However, a comparison of the thermal stability of both redox states of PCa and PCb shows that at neutral pH the reduced proteins are more stable than their oxidized forms, in good agreement with DSC studies (unpublished observations) and with previous CD studies on spinach PC (*7*). Two other experimental findings suggest the conformational unequivalence of both redox states of the proteins. First, their thermal denaturation pathway is different as revealed by temperature-induced IR difference spectroscopy (see Figures 2−4). The intermediate conformation experimentally observed during the thermal unfolding of reduced, but not of oxidized, PC may reflect a rearrangement of the protein conformation that allows H → D exchange. This is also suggested by the absence of such an intermediate in the thermal denaturation pathway of oxidized PC, even when the protein is thermally denatured and extensively exchanges with the solvent. The second evidence comes from the fact that reduced, in contrast to oxidized, PC can partially regain a native-like secondary structure after thermal denaturation.

Our data also demonstrate that lowering the pH to 4.8 has a pronounced effect on the thermal stability of the reduced and oxidized forms of both PC sequences. This is clearly shown by a drastic decrease in the T_m values as compared to those obtained at pH 7.0. The destabilizing effect is greater for reduced PC than for the oxidized form of the protein, reinforcing the existence of conformational differences between both redox states of the protein. This finding,

together with the fact that the secondary structure of both sequences does not significantly change within the pH range studied, points to the pH-sensitivity of the tertiary structure of the protein, in good agreement with near-UV CD studies (*6*).

Redox-Induced Conformational Changes and Electrochemical Properties of PCa and PCb. A comparison between the absorption IR spectra of oxidized and reduced PC indicates that the spectral features especially sensitive to the redox state of the protein are located in the 1700−1610 cm^{-1} spectral region. Reaction-induced IR spectroscopy not only confirms this observation but also allows accurate characterization of subtle redox-induced conformational changes in both H_2O and D_2O media.

The oxidized-minus-reduced infrared spectra shown here display differential features that indicate a conformational transition between two well-defined and distinct protein conformations. Although this finding apparently contradicts previous X-ray results (*4*, *5*), it might be explained by considering that the structural sensitivity of IR spectroscopy can point out conformational differences between two states of a protein even in cases where X-ray crystallography does not show significant changes (*31*). It should also be noted that the small amplitude of the absorbance changes (3−4% of the amide band intensity) suggests that the redox-induced conformational transition is localized, and it might reflect modifications in hydrogen bonding within existing secondary structure elements rather than a net change of secondary structure. This interpretation would be in accordance with NMR studies (*32*) and supports the experimental evidence suggesting that the high ionic strength conditions used in X-ray crystallography could attenuate and even suppress the redox-state-dependent conformational changes (*6*, *7*, *32*, *33*). Possible contributions to the experimentally observed differential signals arise from peptide C═O groups and amino acid side chains. Some of the amino acid residues that could give rise to absorption bands in the 1700−1600 cm^{-1} spectral region include Asn, Gln, and His. The C═O mode of Asn (1680 cm^{-1}) and Gln (1670 cm^{-1}), and the $CN_3H_5^+$ mode of Arg (1673 cm^{-1}) have extinction coefficients comparable to those of the peptide C═O groups (*34*). In contrast, the extinction coefficient of the NH_2^+ mode of His (around 1660 cm^{-1}) is about 20 times weaker than that of the peptide C═O group, and therefore its contribution is expected to be very small.

To distinguish between these two possibilities, it is necessary to analyze the effect of deuteration on the position and intensity of the difference features. The deuteration-induced downshift of signals originating from solvent-exposed side chains of residues such as Asn, Gln, or His is more pronounced ($\geq$30 cm^{-1}) than that expected for peptide C═O groups involved in hydrogen-bonded structures (*22*, *25*, *31*). The experimentally determined displacement of the difference signals, except the positive one at 1650 cm^{-1}, upon deuteration varies from 1 cm^{-1} (1692 cm^{-1}) to 10 cm^{-1} (1629 cm^{-1}), with intermediate values for other spectral features. Although some of these shifts are larger than those observed for other type I copper proteins (*22*; Kaiser et al., unpublished observations), they still remain far from those described for solvent-exposed amino acid side chains. Therefore, we favor the asssignment of these differential signals appearing in the amide I region (1700−1600 cm^{-1}) either to a local change of secondary structure or to a modification of hydrogen bonding to the C═O oxygen within a given secondary structure. These signals most likely represent turns and β strands (1629 cm^{-1}), whose conformation might be important for PC to interact with the appropriate redox partner. The assignment of the positive signal at 1650 cm^{-1}, which is only resolved in H_2O, is not straightforward. Solvent-accessible His residues can be ruled out as possible candidates, since their vibrations should be downshifted by 30−40 cm^{-1} upon deuteration. Alternatively, if the positive difference signal in H_2O were due to buried His residues, the signal would not shift and could merge with the 1665 cm^{-1} signal into one at 1659 cm^{-1} in D_2O. An assignment along this line could explain the higher relative intensity of the resulting band in D_2O. However, due to the small extinction coefficient of this mode, it seems unlikely that the two His residues liganding the copper can cause such a strong difference band. Other probable candidate(s) could be a peptide C═O group(s), whose amide I mode is downshifted by 6−10 cm^{-1} upon deuteration and cancels with a negative band. This band appears as a shoulder at 1641 cm^{-1} in the spectrum recorded in D_2O-based buffer.

In the 1600−1500 cm^{-1} range, the clear difference signal at 1528(−)/1509(+) is slightly downshifted ($\approx$2 cm^{-1}) while its intensity is reduced upon deuteration. This behavior leads to assign this spectral feature to tyrosine C−C ring vibrations (*25*), although a contribution from Lys side chains and peptide N−H modes to the 1528(−) cm^{-1} signal might also explain its weaker amplitude in D_2O. The solvent-exposed Tyr 83, which is surrounded by two negative patches, has been proposed by mutagenesis experiments to play a key role in the reduction of the physiological electron donor cytochrome *f* (*35*, *36*). Therefore, it is reasonable to propose that the above spectral signal is due to modifications in the chemical environment of this residue in response to changes in the redox state of the protein, in agreement with near-UV CD data (*8*).

The clearest redox-dependent spectral change occurs for both sequences at acidic pH. Besides the pattern of differential signals similar to that described at neutral pH, three new bands appear whose amplitude increases as the pH decreases. The broad positive band around 1710−1700 cm^{-1} and the two negative bands at 1567 and 1404 cm^{-1} indicate the protonation of Asp or Glu residue(s) upon plastocyanin oxidation. The intensity of these bands is in agreement with the above assignment, since the extinction coefficients of the COOH ($\approx$1710−1700 cm^{-1}) and the symmetric COO^- (1405 cm^{-1}) modes are similar, whereas that of the antisymmetric COO^- mode (1571 cm^{-1}) is about 2-fold stronger (*25*, *34*). Their bandwidths, close to those found for aqueous solutions of Asp and Glu (*25*), suggest that the residue(s) responsible for the spectral change is (are) located in a solvent-exposed region of the PC molecule. In both acidic patches (residues 42−43 and 59−61) at the "east" face of the PC molecule, the cooperative electrostatic effect of the charge of each residue on the pK_a value of other proximal residues could increase their pK_a value as compared with the intrinsic values expected for the carboxylate groups of Asp and Glu (4.0 and 4.5, respectively), and could couple, as a consequence of a change in the relative position of (a) COO^- group(s) with respect to a charge(s) within the PC

molecule, an increase of its pK_a to the oxidation of the copper center.

It is important to note that similar observations have been made for halocyanin (*22*), another small copper protein that shows little homology with PC. Therefore, it is tempting to propose that the oxidation-associated protonation of an acidic residue(s) could represent a redox-dependent conformational change shared by several members of this type of proteins. An oxidation-linked protonation of an acidic residue(s) could aid dissociation of oxidized PC from PSI, but hinder dissociation of reduced PC from cytochrome *f*.

ACKNOWLEDGMENT

We thank Drs. J. L. R. Arrondo and F. M. Goñi for critically reading the manuscript.

REFERENCES

1. Sigfridsson, K. (1998) *Photosynth. Res. 57*, 1−28.
2. Redinbo, M. R., Yeates, T. O., and Merchant, S. (1994) *J. Bioenerg. Biomembr. 26*, 49−66.
3. Ort, D. R., and Melandri, A. (1982) In *Photosynthesis, Volume I: Energy Conversion by Plants and Bacteria* (Govindjee, E., Ed.) pp 539−589, Academic Press, Inc., New York.
4. Guss, J. M., and Freeman, H. C. (1983) *J. Mol. Biol. 169*, 521−563.
5. Guss, J. M., Harrowell, P. R., Murata, M., Norris, V. A., and Freeman, H. C. (1986) *J. Mol. Biol. 192*, 361−387.
6. Draheim, J. E., Andersson, G. P., Duane, J. W. and Gross, E. L. (1986) *Biophys. J. 49*, 891−900.
7. Gross, E. L., Draheim, J. E., Curtis, A. S., Crombie, B., Scheffer, A., Pan, B., Chiang, C., and López, A. (1992) *Arch. Biochem. Biophys. 298*, 413−419.
8. Durell, S. R., Labanowski, J. K., and Gross, E. L. (1990) *Arch. Biochem. Biophys. 277*, 241−254.
9. Dimitrov, M. I., Egorov, C. A., Donchev, A. A. and Anatosov, B. P. (1987) *FEBS Lett. 226*, 17−22.
10. Arrondo, J. L. R., Castresana, J., Valpuesta, J. M., and Goñi, F. M. (1994) *Biochemistry 33*, 11650−11655.
11. Baymann, F., Moss, D. A., and Mäntele, W. (1991) *Anal. Biochem. 199*, 269−274.
12. Hill, H. A. O., Page, D. J., Walton, N. J., and Whitford, D. (1985) *J. Electroanal. Chem. Interfacial Electrochem. 187*, 315−324.
13. Fritz, F., Moss, D. A., and Mäntele, W. (1991) *FEBS Lett. 297*, 167−170.
14. Mäntele, W. (1996) in *Biophysical Techniques in Photosynthesis* (Hoff, A., and Amesz, J., Eds.) pp 137−160, Kluwer, Dordrecht.
15. Susi, H. (1969) in *Structure and Stability of Biological Macromolecules* (Timasheff, S. N., and Stevens, L., Eds.) pp 575−663, Dekker, New York.
16. Krimm, S., and Bandekar, J. (1986) *Adv. Protein Chem. 38*, 181−364.
17. Arrondo, J. L. R., Castresana, J., Muga, A., and Goñi, F. M. (1993) *Prog. Biophys. Mol. Biol. 59*, 23−56.
18. Surewicz, W. K., Mantsch, H. H., and Chapman, D. (1993) *Biochemistry 32*, 389−394.
19. Chirgadze, Y. N., Fedorov, O. V., and Trushina, N. P. (1975) *Biopolymers 14*, 679−694.
20. Fabian, H., Schultz, C., Naumann, D., Landt, O., Hahn, U., and Saenger, W. (1993) *J. Mol. Biol. 232*, 967−981.
21. Martinez, A., Haavik, J., Flatmark, T., Arrondo, J. L. R., and Muga, A. (1996) *J. Biol. Chem. 271*, 19737−19742.
22. Brischwein, M., Scharf, B., Engelhard, M., and Mäntele, W. (1993) *Biochemistry 32*, 13710−13717.
23. Sykes, A. G. (1991) *Struct. Bonding (Berlin) 75*, 175−224.
24. Surewicz, W. K., Szabo, A. G., and Mantsch, H. H. (1987) *Eur. J. Biochem. 167*, 519−523.
25. Venyaminov, S. Y., and Kalnin, N. N. (1990) *Biopolymers 30*, 1243−1257.
26. Orengo, C. A., Michie, A. D., Jones, S., Jones, D. T., Swindells, M. B., and Thornton, J. M. (1997) *Structure 5*, 1093−1108.
27. Fabian, H., Naumann, D., Misselwitz, R., Ristan, O., Gerlach, D., and Werfle, H. (1991) *Biochemistry 30*, 10479−10485.
28. Urbanova, M., Dukor, R. K., Pancoska, P., Fupta, V. P., and Keiderling, T. A. (1991) *Biochemistry 30*, 10479−10485.
29. Bañuelos, S., and Muga, A. (1995) *J. Biol. Chem. 270*, 29910−29915.
30. Valencia, A., Hubbard, T. J., Muga, A., Bañuelos, S., Llorca, O., Carrascosa, J. L., and Valpuesta, J. M. (1995) *Proteins: Struct., Funct., Genet. 22*, 199−209.
31. Mäntele, W. (1993) *Trends Biochem. Sci. 18*, 197−202.
32. Ulrich, E. L., and Markley, J. L. (1978) *Coord. Chem. Rev. 27*, 109−140.
33. Draheim, J. E., Anderson, G. P., Pan, R. L., Rellick, L. M., Duane, J. W., and Gross, E. L. (1985) *Arch. Biochem. Biophys. 237*, 110−117.
34. Venyaminov, S. Y., and Kalnin, N. N. (1990) *Biopolymers 30*, 1259−1271.
35. He, S., Modi, S., Bendall, D. S. and Gray, J. C. (1991) *EMBO J. 10*, 4011−4016.
36. Kannt, A., Young, S., and Bendall, D. S. (1996) *Biochim. Biophys. Acta 1277*, 115−126.

BI990376T